ANALES de Edificación

Received: 7/03/2024
Accepted:17/03/2024

Anales de Edificación
Vol. 10, Nº1, 45-53 (2024)
ISSN: 2444-1309
DOI: 10.20868/ade.2024.5387

Evolución del índice de estrés por calor de la ciudad de Madrid mediante el modelo climático UrbClim de la Agencia Espacial Europea

Evolution of the heat stress index of the city of Madrid using the URBCLIM climate model of the European Space Agency

David Hidalgo García[a]

[a] Departamento de Expresión Gráfica Arquitectónica y en la Ingeniería. E.T.S. Ingeniería de Edificación. Universidad de Granada. dhidalgo@ugr.es

Resumen-- **El calentamiento global está generando importantes incrementos de la temperatura ambiental que está afectando a la calidad de vida de las personas. Hoy en día, el 30% de la población mundial reside en lugares que cuentan con condiciones climáticas de calor extremo y se espera que se incremente al 74% en las próximas dos décadas. En esta investigación se ha analizado la evolución que ha experimentado el índice de estrés por calor (Hi) entre los años 2008, 2012 y 2017 en las diferentes Zonas Climáticas Locales (ZCL) de la ciudad de Madrid mediante el modelo climático UrbClim de la Agencia Espacial Europea. Mediante imágenes satelitales Landsat 5 y 8 y para cada ZCL, se han tenido en cuenta las siguientes variables: Índice de vegetación de diferencia normalizada y el índice de edificación de diferencia normalizada. Nuestros resultados reportan que se ha producido entre los años un importante crecimiento de los valores de estrés por calor siendo mayor en las ZCL de uso urbano (ZCL-2, 3, 4, 5, 6, 8 y 9) y menor en las ZCL de uso rural (ZCL-A, B, C, D, E, F y G). Por tanto, es necesario el aumento de zonas y espacios verdes y el empleo de fachadas y cubiertas vegetales en las zonas urbanas al objeto de aumentar la resistencia al calor de las areas urbanas.**

Palabras clave— Índice de estrés por calor; modelo UrbClim; zonas climáticas locales; mitigación del calor; clima urbano.

Abstract— **Global warming is generating significant increases in environmental temperature that is affecting people's quality of life. Today, 30% of the world's population resides in places that have extreme heat weather conditions, and this is expected to increase to 74% in the next two decades. In this research, the evolution of the heat stress index (Hi) between 2008, 2012 and 2017 in the different Local Climate Zones (LZs) of the city of Madrid has been analysed using the UrbClim climate model of the European Space Agency. Using Landsat 5 and 8 satellite images and for each ZCL, the following variables have been considered: Normalized Difference Vegetation Index and the Normalized Difference Building Index.. Our results report that there has been a significant increase in heat stress values between the years, being higher in the ZCL-2, 3, 4, 5, 6, 8 and 9 and lower in the ZCL-for rural use (ZCL-A, B, C, D, E, F and G). Therefore, it is necessary to increase green areas and spaces and the use of facades and green roofs in urban areas in order to increase the heat resistance of urban areas.**

Index Terms— Heat stress index; UrbClam model; local climate zones; heat mitigation; urban climate.

I. INTRODUCTION

One of the most urgent and necessary issues currently facing society is climate due to global warming and extreme events (Kovats *et al.,* 2005; Song *et al.,* 2020; An *et al.,* 2020; Founda & Santamouris, 2017). The fifth report of the Intergovernmental Panel on Climate Change (IPCC) has shown that in recent decades there has been a significant increase in

D.H.G is PhD student at Architectural and Engineering Graphic Drawing at Escuela Técnica Superior de Ingeniería de la Edificación, Universidad de Granada, (Spain)

ambient temperatures that will lead to significant negative effects on the health and quality of life of inhabitants, mainly in urban areas (IPCC, 2013). The transformation of land cover caused by the growth of urban areas generated by the significant increase in population is one of the procedures that most favors climate change and the increase in global temperatures (Song *et al.,* 2020; Li *et al.,* 2011). Transformations of the cover decrease evapotranspiration (Stewart & Oke, 2012) due to the increase in surfaces and spaces built with impermeable materials. During the day, they store the heat received from solar radiation and in the evening they release it into the atmosphere (An *et al.,* 2020; Arnfield, 2003; Zhou *et al.,* 2015), increasing the ambient temperature. It is estimated that this situation will continue to increase, as the latest forecasts from the United Nations (UN) foresee an increase in the urban population by 20% by 2050 (UNO, 2018), which will imply a significant transformation of global urban coverage (Schneider *et al.,* 2010). Some studies have reported positive correlations between urban areas and ambient temperatures and negative correlations between the latter and green areas. Thus, urban areas have higher temperatures than rural areas, but green spaces in urban areas also have lower temperatures than urbanized areas (Hidalgo García & Arco Díaz, 2021; Hua *et al.,* 2020; Karakuş, 2019; Guo *et al.,* 2020). At the same time, the increase in temperatures in urban areas is increased by the Urban Heat Island (ICU) phenomenon. This is a phenomenon of modification of the urban climate and its persistence is affected by different human tasks (Santamouris, 2020).

Today, it is estimated that 30% of the world's population suffers from extreme heat weather conditions and the forecast is that in the next 20 years this will reach 74% (Mora *et al.,* 2017). Faced with this climate emergency, it is considered necessary to carry out studies to identify which areas of cities are more likely to suffer from severe heat stress, when these levels of heat could be reached and what factors influence their growth. All this, with the aim of adopting measures that protect citizens and improve their quality of life through the determination of guidelines and the taking of measures by urban planners and public administrations. To measure the heat exposure that urban dwellers may have and within the scientific community, the heat stress index (Hi) is commonly used (Kotharkar *et al.,* 2021; Jacobs *et al.,* 2019; Verdonck *et al.,* 2018) since it obtains adequate results with environmental conditions and only requires two parameters: ambient temperature and relative humidity. To understand and obtain these environmental variables, it is possible to use urban climate models such as the Muklimo of the German meteorological agency (Geletič *et al.,* 2018) or the UrbClim of the Copernicus climate change service (Verdonck *et al.,* 2018; Martí Ezpeleta & Royé, 2021; De Ridder *et al.,* 2015) attached to the European Space Agency (ESA). This consists of a simple urban surface energy balance model designed to target the spatial scale of a city, but fast and comprehensive enough to obtain results with high levels of accuracy (De Ridder *et al.,* 2015). Its use in heat stress studies in urban areas is widespread (Verdonck *et al.,* 2018; Royé *et al.,* 2021) as it allows climatic variables to be obtained at a resolution of 100 meters.

Existing studies of heat stress in urban areas and its evolution over the last few decades have reported that it has increased significantly, has a high spatio-temporal variability and is conditioned by the climatic and morphological conditions of cities. Thus, the heat stress index is higher during the summer months and is more intense in urban areas with high densities and few green areas (Kotharkar *et al.,* 2021; Jacobs *et al.,* 2019; Geletič *et al.,* 2018; Kumar *et al.,* 2022; Hass *et al.,* 2016). Thus, the study of heat stress in the city of Madrid using the UrbClim model between 2008 and 2017 reported an important positive correlation between the different coverages and heat stress (Royé *et al.,* 2021). Studies on four cities (Kolkata, Chennai, Delhi, Mumbai) in India (Kumar *et al.,* 2022) and on the city of Nagpur (India) (Kotharkar *et al.,* 2021) reported that the increase in heat stress is greater in areas with higher density and population as opposed to neighborhoods with lower density and population where the increase in stress is lower. On the other hand, and taking into account the ZCLs, the heat stress studies on the cities of Nagpur (India) (Kotharkar *et al.,* 2021), Brno (Czech Republic) (Geletič *et al.,* 2018) and Antwerp, Brussels and Ghent (Belgium) (Verdonck *et al.,* 2018) reported that the ZCLs identified as 2, 3, 5, 8, 9 and 10 presented a higher heat stress while the ZCL 6, B, D and G had lower heat stress due to the greater availability of green areas and fewer impervious areas.

The aim of this research is to analyze the evolution of the heat stress index (Hi) during the years 2008, 2012 and 2017 in the different ZCL of the city of Madrid using the UrbClim climate model. With the help of Landsat 5 and 8 images, the Normalized Built-Up Difference Index (NDBI) and the Normalized Difference Vegetation Index (NDVI) have been generated, and the World Urban Database and Access Portal Tools (WUDAPT) atlas have obtained the different ZCLs. Then, with the help of statistical analysis and using the Data Panel and ANOVA techniques, the correlations between the data obtained and the relationship between the variables have been determined.

The questions that we propose to answer with this research are the following: 1. What evolution has the heat stress index experienced between 2008, 2012 and 2017 in the city of Madrid? 2. Is there a relationship between the heat stress index and the NDVI and NDBI indices in the different ZCLs? 3. Can the results obtained be important in future urban planning of urban areas?

The advance provided by this study is to facilitate a study on the evolution of the heat stress index on the different LCZs during the years 2008, 2012 and 2017 and what factors influence its variability. All this with the aim of improving future decisions by urban planners and public administrations on the development of new urban areas. The predilection for the development of heat stress-resilient ZCLs will enable urban areas to become climate-resilient environments and improve people's quality of life. All this, through a methodology under an open-source work environment to be able to extrapolate the results obtained to other areas.

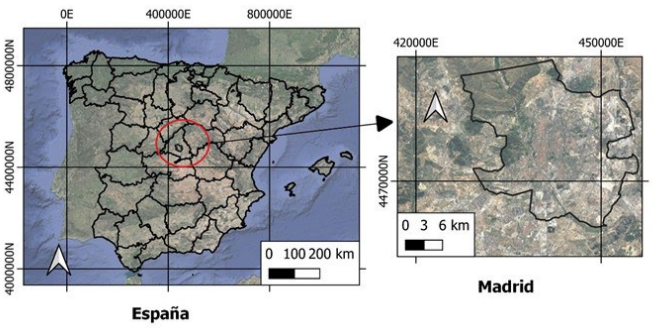

Fig. 1: City of Madrid, Spain. (Source: Authors' own elaboration on Google maps)

II. Methods

A. Study area

The city of Madrid is shown in Fig. 1. The UTM geographical coordinates are latitude 37º 20' 44.54" and longitude 5º 58' 16.62". The altitude above sea level is 657 m. Its population is 3.22 million. The climate according to the Köppen-Geiger climate classification is of the Mediterranean climate type (Csa). This implies hot, dry summers and wet, cold winters (de Castro *et al.,* 2007).

B. Methodology

First, the NDVI and NDBI indices of the city of Madrid have been obtained using Landsat 5 images (2008) with a resolution of 30 meters and using Landsat 8 (years 2012 and 2017) with a resolution of 15 meters. The high-precision drawings of the different ZCLs from the WUDAPT atlas have been downloaded below. This database is supported by observation and numerical modeling values for the different thermal characteristics of cities [20,27]. Its use in soil identification studies using ZCL is widely documented [20,28,29]. The average values of relative humidity and ambient temperature for the month of August for the years 2008, 2012 and 2017 have been obtained from the UrbClim model of the European Space Agency (ESA). With these data, the heat stress index has been obtained in the different ZCLs and subsequently correlated with the rest of the indices with the help of statistical analysis using the specialized software for data science, STATA, version 16. ANOVA analysis and data panel were used to determine and analyze significant correlations of the variables.

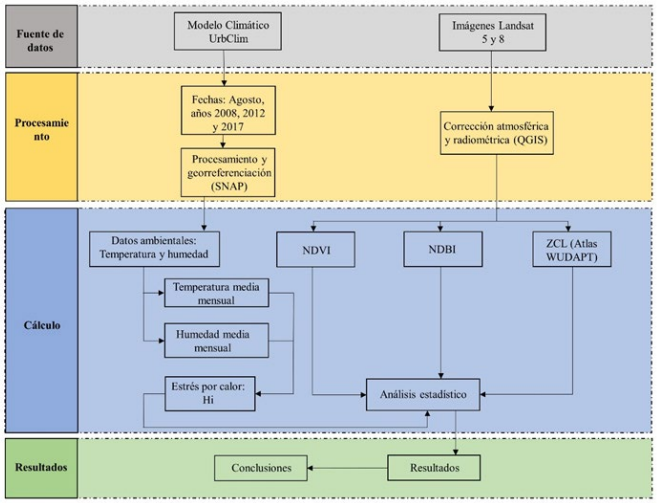

Fig. 2. Flow chart designed. Source: Author's creation.

C. Landsat Images

Landsat 5 and 8 images were obtained from the United States Geological Survey (USGS) for the years 2008, 2012, and 2017, respectively. The Landsat 5 satellite has a total of seven multispectral bands with a resolution ranging from 120 to 30 meters. In contrast, Landsat 8 has ten bands with a resolution ranging from 100 to 15 meters. The images selected for this research correspond to the month of August of the years 2008, 2012 and 2017. It was considered that the cloudiness of the selected days was not greater than 5% to increase the uptake of urban areas. After downloading, the images underwent an atmospheric correction process in OLI bands. To this end, the Dark Object Subtraction (DOS) algorithm was used (Chavez, 1988; Zhang *et al.,* 2015) and the Semi-Automatic Classification (SPC) plugin implemented in the QGIS software was used (Congedo, 2016; Rozenstein *et al.,* 2014).

NDVI makes it possible to determine the greenness and density of vegetation using the near-infrared (NIR) and red (Red) spectral bands. The result gives us a range of values ranging from -1 to 1. It is calculated using equation 1:

$$NDVI = \frac{NIR - Red}{NIR + Red} \quad (1)$$

Using the NDBI we can determine the proportion of built-up areas compared to non-built areas. The result gives us a range of values ranging from -1 to 1. It was calculated using the shortwave infrared (SWIR) and near-infrared (NIR) bands according to equation 2 (Zha *et al.,* 2003):

$$NDBI = \frac{NIR - SWIR}{NIR + SWIR} \quad (2)$$

D. ZCL Mapping & Classification

The ZCL maps of the city of Madrid (Fig. 3) are found in the WUDAPT atlas database (Verdonck *et al.,* 2018; Demuzere *et al.,* 2022) (https://ZCL-generator.rub.de/submissions) based on the classification proposed by the authors Steward and Oke (2009). The identification of the different ZCLs makes it possible to catalogue areas that have a specific thermal regime over time based on their location and morphological characteristics (Stewart & Oke, 2012). Its use in landscape

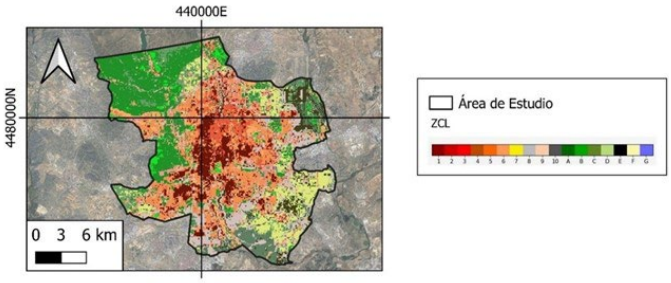

Fig. 3: ZCL established for the city of Madrid according to Atlas WUDAPT. (Source: https://ZCL-generator.rub.de/submissions)

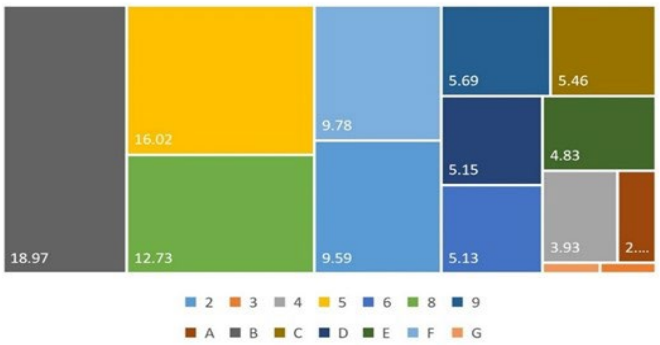

Fig. 4: % of surface area of each ZCL in the city of Madrid. (Source: Authors' own elaboration with WUDAPT atlas data)

characterization studies is widely documented (Anjos *et al.,* 2020; Emmanuel & Krüger, 2012; Wang & Ouyang, 2017; Brousse *et al.,* 2019; Khamchiangta & Dhakal, 2019; Equere *et al.,* 2020). Fig. 4 shows the area (%) occupied by each ZCL. Thus, the ZCLs with the greatest extension are 2, 5, 8 and 4, while those with the smallest extension are G, 3, E and D.

The accuracy values reported by the WUDAPT atlas for the cities investigated range from 0.67 to 0.69. However, a qualitative and quantitative comparison of the different LCZs was made with Landsat and Google Street View satellite imagery. In general, the ZCLs of the atlas are consistent with satellite imagery and Google Street View, presenting values that fall within the patterns defined by the authors Steward and Oke, (2012).

E. UrbClum Model

Average ambient temperature and relative humidity data for the months of August for the years 2008, 2012 and 2017 were obtained from the UrbClim model developed by ESA's Copernicus programme. This model, commonly used in similar research, is based on a transfer scheme between the two affected layers: atmosphere and geosphere (De Ridder *et al.,* 2015). This scheme, initially called the Land Surface Interaction Calculation (LAICA), only included rural areas, but was later modified to include urban areas (De Ridder *et al.,* 2015). Its use in climate studies on urban spaces has been validated by studies carried out in several European cities, such as Antwerp, Bruges, Ghent (Verdonck *et al.,* 2018) and Madrid (Martí Ezpeleta & Royé, 2021).

F. Hi (heat index)

Equation 3 has been used to determine the Hi in the cities investigated. This was developed in 1990 (Rothfusz, 1990) and later modified (Brooke Anderson *et al.,* 2013) according to formula 5:

$$\begin{aligned} Heat\ Index\ (Hi) = & -8.78469475556 + (1.61139411 \times T) \\ & + (2.33854883889 \times H) \\ & - (0.14611605 \times T \times H) \\ & - (0.012308094 \times T^2) \\ & - (0.0164248277778 \times H^2) \\ & + (0.002211732 \times T^2 \times H) \\ & + (0.00072546 \times T \times H^2) \\ & - (0.000003582 \times T^2 \times H^2) \end{aligned} \quad (3)$$

TABLE I
CLASSIFICATION OF THE HEAT STRESS INDEX (HI) AND EFFECTS ON THE POPULATION.

Heat Index	Heat Rating	Hi	Overall effect on people
Hi-1	Risk-free	< 26.00	There is no risk to the population group.
Hi-2	Very warm	26.66 – 32.21	Fatigue possible with prolonged exposure and physical activity.
Hi-3	Hot	32.22 - 39.43	Heat stroke, heat cramps or heat exhaustion LIKELY and heat stroke POSSIBLE with prolonged exposure and/or physical activity.
Hi-4	Very hot	39.44 - 51.10	Heat stroke, heat cramps, or heat exhaustion POSSIBLE with prolonged exposure and/or physical activity.
Hi-5	Extremely hot	>51.11	Heat/heat stroke VERY LIKELY with continuous exposure.

Where: Hi is the heat stress index in °C, T is the air temperature in °C, and H is the relative humidity in %. Based on the results obtained, the effects of heat on the population can be determined based on Table 1 (Kotharkar *et al.,* 2021).

III. RESULTS

A. Evaluation of NDVI and NDBI indices

The spatio-temporal evolution of the NDVI and NDBI indices of the city of Madrid during the years 2008, 2012 and 2017 can be consulted in Figs. 5 and 6.

The average results of the NDVI and NDBI indices for each year investigated can be shown in Fig. 7. The results obtained correspond to the standard values for a city with this geographical location, characteristics and population. The NDVI values indicate that the vegetation can be considered as dispersed and suitable for the summer period, considering that the selected satellite images correspond to the summer season. The NDVI in 2012 is higher than in 2008 while in 2017 it decreases compared to 2012. This circumstance could be motivated by the geographical location of the city and its relationship with the rainfall that influences the state of the vegetation.

The NDBI values suggest that in Madrid compact areas with a medium-high density predominate, as opposed to open areas with low-medium density and green areas. There has been a significant increase in built-up areas between 2008 and 2017. It is interesting to note how in Madrid the increase coincides with the significant decrease in the value of the NDVI index. This circumstance could be motivated by the development of large compact built-up areas that have smaller areas for green areas than open areas. Numerous studies report negative relationships between NDVI and NDBI indices in urban areas that have experienced significant growth (Kafy *et al.,* 2021; Wang *et al.,* 2019; Yang *et al.,* 2020).

Fig. 8 shows the mean values of NDVI and NDBI in each ZCL. In general terms, the NDVI index presents the highest values in the ZCLs classified as rural (A, B, C, D, E, F and G). On the contrary, the lowest values are reported in the ZCLs

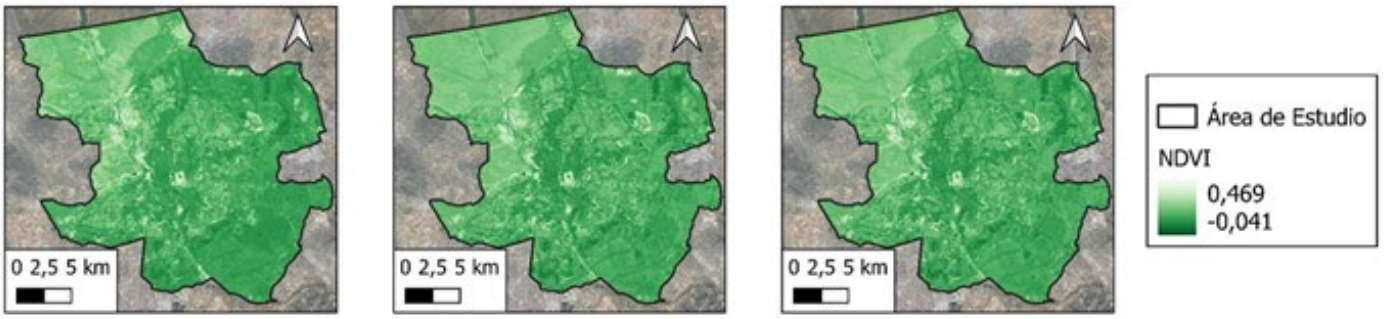

Fig. 5: Evolution of NDVI Madrid 2008, 2012 and 2017. (Source: Authors' own elaboration with Landsat 5 and 8)

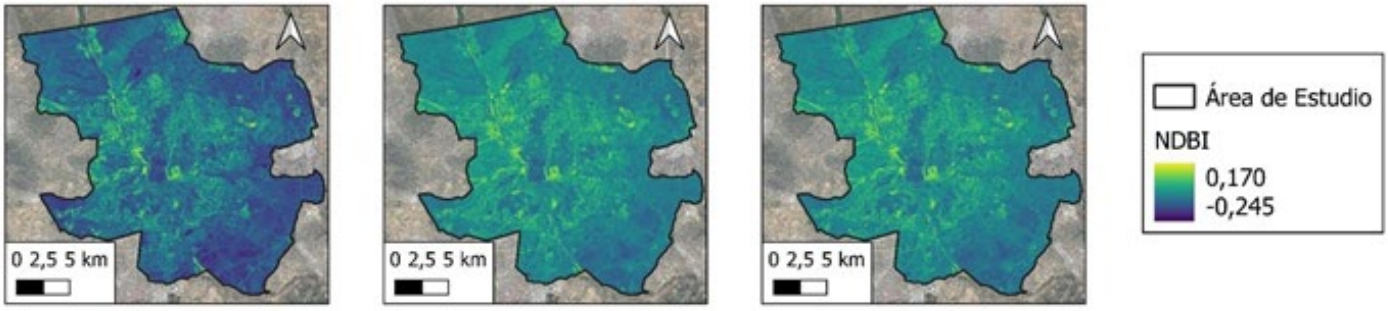

Fig. 6: Evolution of NDBI Madrid 2008, 2012 and 2017. (Source: Authors' own elaboration with Landsat 5 and 8)

classified as urban (2, 3, 4, 5, 6, 8 and 9). Within urban areas, open ZCLs (4, 5 and 6) present higher NDVI values as opposed to the lower values obtained in compact ZCLs (2 and 3). These data suggest that vegetation is lusher and has a larger surface area in rural areas and open urban areas as opposed to compact urban areas.

On the other hand, the NDBI index has the highest values in urban ZCLs (2, 3, 4, 5, 6, 8 and 9) as opposed to the lowest values obtained in rural ZCLs (A, B, C, D, E, F and G). Within urban areas, compact ZCLs (2 and 3) present higher values as opposed to the lower values obtained in open ZCLs (4, 5 and 6). These data suggest that buildings are more occupied and denser in urban areas as opposed to rural areas and within the former in compact areas as opposed to open areas.

The results of the ANOVA test carried out on the NDVI and NDBI indices showed through the Shapiro Wilk test that they present non-normal distributions within the different ZCL since P value < 0.05. Therefore, to continue with the ANOVA analysis for non-normal distributions, it is necessary to perform the Kruskal Wallis test, the results of which are shown in Table 2. According to these reported results, the NDVI and NDBI indices present statistically significant relationships above 99% in the different ZCLs of the cities investigated.

B. Heat stress index

Fig. 9 shows the spatio-temporal evolution of Hi temperatures in the city of Madrid between 2008, 2012 and 2017. Hi values are higher in urban areas (those with higher NDBI index values and lower NDVI index values) as opposed to rural areas (those with higher NDVI index values and lower NDBI index values) where Hi values are lower.

Fig. 10 shows the average evolution of the Hi index by year for the city of Madrid. In general terms, there is an increasing

TABLE II
ANOVA TEST RESULTS OF THE NDVI AND NDBI INDICES IN THE DIFFERENT ZCLS

Data	NDVI	NDBI
P value	0,0001***	0,0001***
F	1253,453	869,260

F: Statitian

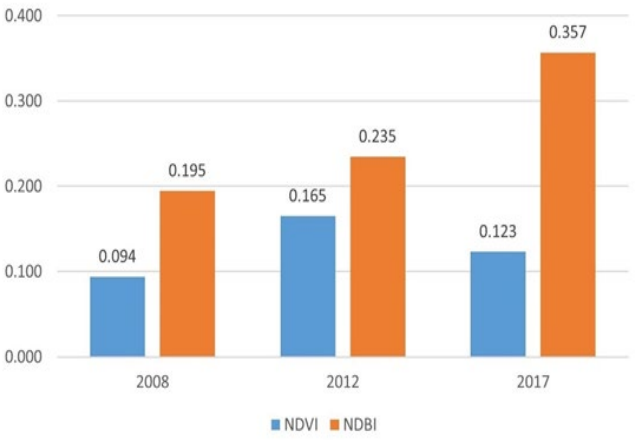

Fig. 7: Evolution of NDVI and NDBI indices Madrid years 2008, 2012 and 2017. (Source: Authors)

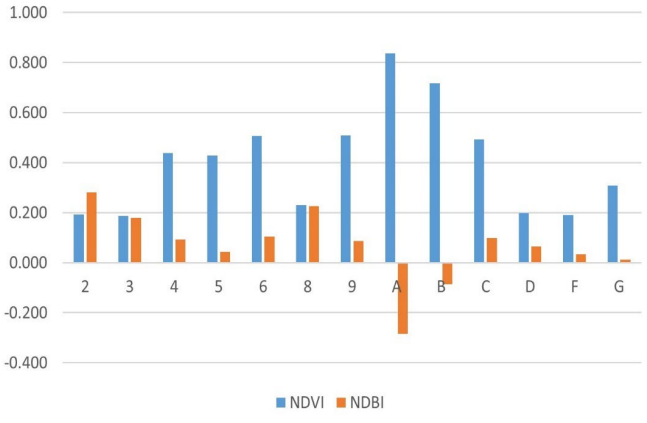

Fig. 8: Average NDVI and NDBI index values for each ZCL in Madrid. (Source: Authors' own elaboration with Landsat 5 and 8 images)

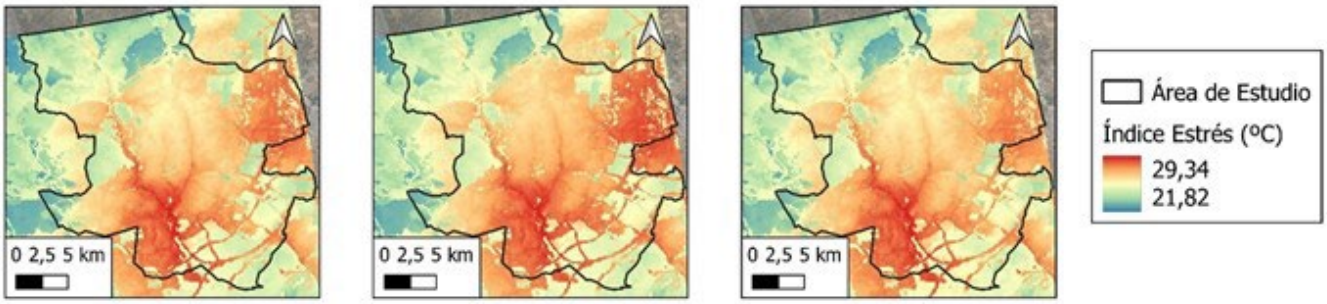

Fig. 9: Evolution of the Hi Madrid Index in 2008, 2012 and 2017. (Source: Authors' own elaboration with UrbCLim data)

trend in the Hi index obtained in the different years investigated. Thus, in 2008 the average value of Hi in Madrid was 26.33ºC while in 2017 it was 28.2ºC. These values report an average growth of 7.10% between the two years. The high increase in the Hi could be justified by its high urban growth, corroborated by the increase in the NDBI index and the decrease in the NDVI index.

Fig. 11 shows how the classification of the Hi index has evolved between 2008 and 2017 according to the effects on the population (Table 1). In this way, it can be seen how the area classified as no risk has been reduced and even disappeared in 2012 and the area classified as warm has increased, especially in 2017.

Fig. 12 shows the evolution of the Hi index for each ZCL. It can be observed that the greatest increases in Hi occur in urban ZCLs (2, 3, 4, 5, 6, 8 and 9) while on the contrary, the increases are smaller in rural ZCLs (A, B, C, D, E, F and G). Thus, the city has experienced an average growth of Hi in urban ZCLs of 3.46% while the growth in rural ZCLs has been 2.91%. It can also be seen that within urban areas, compact ZCLs (2 and 3) show greater increases in Hi (3.71%) than open ZCLs (4, 5 and 6) (3.41%).

The results of the ANOVA test carried out on the Hi index showed through the Shapiro Wilk test that they do not present normal distributions within the different ZCL since P value < 0.05. Therefore, in order to continue with the ANOVA test for non-normal distributions, it is necessary to perform the Kruskal Wallis test, the results of which are shown in Table 3.

According to the results reported, the Hi values present statistically significant relationships above 99% between the different ZCLs. Then, in order to determine the relationships between Hi and the NDVI, NDBI and ZCL indices of the cities under study, the statistical analysis is carried out using the Data Panel method. To do this, Pearson's correlation coefficient was first determined and then the analysis called Data Panel was carried out. For the latter, the Generalized Least Squares method was used. The results of the data analysis are shown in Tables 4 and 5.

Table 4 shows that Hi shows a positive correlation with the NDBI index (0.051) and a negative correlation with the NDVI index (-0.316) and ZCL (-0.307).

The results of the statistical analysis using the Data Panel technique (Table 5) show a statistically significant and positive relationship above 99% between the Hi variable and the NDBI variables and a negative relationship above 99% with the NDVI

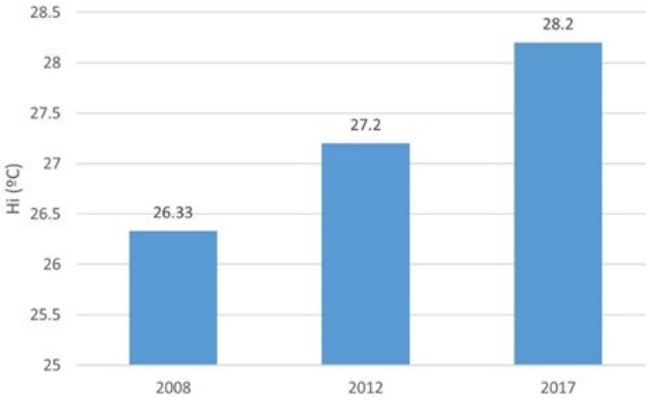

Fig. 10: Average evolution of the Hi index for the years 2008, 2012 and 2017. (Source: Authors' own elaboration with UrbClim data)

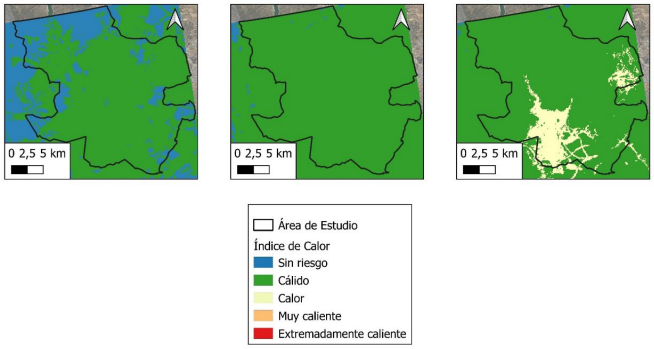

. 11: Evolution of the effects on the Hi index population 2008, 2012 and 2017. (Source: Authors' own elaboration with UrbClim data)

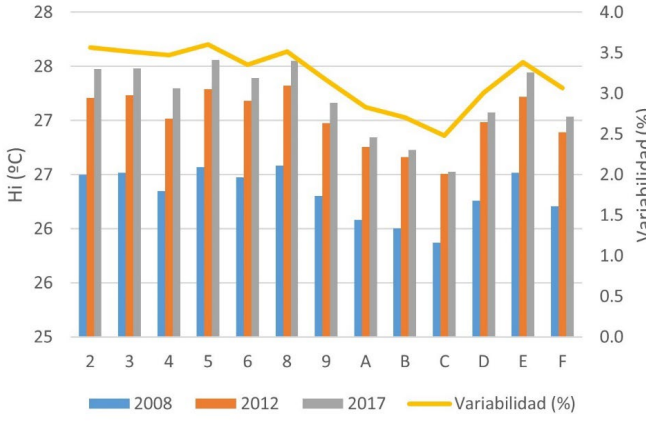

Fig. 12: Evolution of Hi by ZCL. (Source: Authors' own elaboration with data from the UrbClim)

and ZCL variables. It is observed that there is a good agreement between the dependent variable and the independent variables by observing the values of R2, F and Prob>Chi2. The level of fit is greater than 99% significance since Prob>Chi2= 0.000.

IV. Discussion

This study analysed the evolution of the Hi heat stress index during the years 2008, 2012 and 2017 in the city of Madrid and its relationship with the NDVI, NDBI and ZCL indices. All of this is motivated by the need to know the evolution of the Hi and thus obtain a global vision of it that allows the decree of mitigation measures because of climate change and temperature increases.

It has been evidenced that the NDVI index related to vegetation has shown a decrease in the city of Madrid. On the other hand, the results report that the highest values of this index are present in rural ZCLs (A, B, C, D, E, F and G) as opposed to urban ZCLs (2, 4, 5, 6, 8 and 9). However, within urban ZCLs, NDVI values are higher in those classified as open (4, 5 and 6) as opposed to compact ones (2 and 3) where the values are lower. On the contrary, it has been shown that the NDBI index, related to building, has experienced large increases between 2008 and 2017 due to the significant urban development that Spanish cities have experienced. On the other hand, the results report that the highest values of this index are present in urban ZCLs (2, 4, 5, 6, 8 and 9) as opposed to rural ZCLs (A, B, C, D, E, F and G). However, within urban ZCLs, NDBI values are higher in those classified as compact (2 and 3) as opposed to open ones (4, 5 and 6) where the values are lower. These values determine the urban morphology of the city and ZCL studied, and the results are in line with other studies carried out by other authors (Hidalgo García & Arco Díaz, 2021; Wang *et al.,* 2019; Diallo-Dudek *et al.,* 2015; Kafy *et al.,* 2021; Avdan & Jovanovska, 2016) in other cities and territories, allowing the data obtained in this research to be validated. These studies report results that mainly relate low NDVI index values with high NDBI index values in compact urban areas. Conversely, high NDVI values are related to low NDBI values in rural areas. However, the variability obtained in the NDVI indices could not only be attributed to urban planning systems but also, to a small extent, to the variability in rainfall in the area during the period under study (Nicholson & Farrar, 1994; Li *et al.,* 2002).

There has been a significant increase in the Hi heat stress index in the city between 2008 and 2017. However, our results suggest that the Hi index has grown more strongly in urban areas as opposed to rural areas. In relation to the former, this growth has been greater in the compact ZCLs (2 and 3) as opposed to the open ZCLs (4, 5 and 6). This circumstance is due to the use of impermeable materials with high thermal absorption and the scarcity of green areas in compact areas. This produces an increase in ambient temperatures, decreases the relative humidity of the environment, which produces an increase in the Hi index. The arrangement of the green areas allows the minimization of temperatures because of the shadows they generate and the cooling rates due to the evapotranspiration process. Compact urban areas have few green areas and large built-up areas, which gives low NDVI index values and high NDBI index values. This trend has been observed and reported in studies on the cities of Kolkata, Chennai, Delhi, Mumbai and Nagpur (India) where they relate the areas with the largest built-up area and the lowest vegetation cover with the hottest areas and with the highest intensity of the Hi index (Kotharkar *et al.,* 2021; Kumar *et al.,* 2022). At the same time, our results are in line with the research carried out by other authors (Verdonck *et al.,* 2018; Geletič *et al.,* 2018; Martí Ezpeleta & Royé, 2021). The regression model reported statistically significant and negative relationships between the Hi and the NDVI and ZCL indices and positive relationships with the NDBI variable, evidencing what was reported analytically.

TABLE III
ANOVA test results of the NDVI and NDBI indices in the different ZCLs

Data	Hi
P value	0,0001***
F	871,268

TABLE IV
Pearson's correlation coefficient between Hi and NDVI, NDBI and ZCL indices

	Hi	NDVI	NDBI	ZCL
Hi	1			
NDVI	-0,316	1		
NDBI	0,051	-0,693	1	
ZCL	-0,307	0,287	-0,119	1
	Hi	NDVI	NDBI	ZCL

TABLE V
Data Panel between Hi and NDVI, NDBI and ZCL

Variables	β coeficiente	ρ value	Standard deviation
NDVI	-7.608	0.000***	0.362
NDBI	4.525	0.000***	0.326
ZCL	-0.068	0.000***	0.051
	R2=0.69	F=286,21	Prob>chi2= 0.000

V. Conclusions

This study has analysed the evolution of the Hi heat stress index in the city of Madrid during the years 2008, 2012 and 2017. Environmental data have been obtained from ESA's UrbClim climate model. However, to improve the evaluation and allow an extrapolation of the results to other cities, the results have been reported using the widely known classification of land areas of ZCL.

A significant spatio-temporal variability between the Hi and the different LCZs has been corroborated. Thus, urban and compact LCZs (2 and 3) show greater increases in Hi than rural areas and open urban areas (4, 5 and 6). A positive correlation between the Hi and the NDBI and ZCL indices and a negative correlation with the NDVI index have been reported. Therefore, areas with more impervious areas and fewer green areas are more susceptible to greater increases in heat stress.

These circumstances show that public administrations and urban planners should have a predilection in future developments for open ZCLs with large green spaces as opposed to compact ZCLs in order to improve the resilience of cities to future increases in temperatures and Hi. On the other hand, and to improve the quality of life of the inhabitants of existing compact areas, it is necessary to draw up contingency plans and control of the future urban climate that reward the use of green roofs and facades. These results can be extrapolated to other cities or urban areas with the same ZCLs

REFERENCES

An N, Dou J, González-Cruz JE, Bornstein RD, Miao S, Li L. An observational case study of synergies between an intense heat wave and the urban heat island in Beijing. Journal of Applied Meteorology and Climatology. (2020); 59:605–20.

Anjos M, Targino AC, Krecl P, Oukawa GY, Braga RF. Analysis of the urban heat island under different synoptic patterns using local climate zones. Building and Environment. (2020); 185.

Arnfield AJ. Two decades of urban climate research: A review of turbulence, exchanges of energy and water, and the urban heat island. International Journal of Climatology. (2003); 23:1–26.

Avdan U, Jovanovska G. Algorithm for automated mapping of land surface temperature using LANDSAT 8 satellite data. Journal of Sensors. (2016);20 16-23.

Brooke Anderson G, Bell ML, Peng RD. Methods to calculate the heat index as an exposure metric in environmental health research. Environmental Health Perspectives. (2013); 121:1111–9.

Brousse O, Georganos S, Demuzere M, Vanhuysse S, Wouters H, Wolff E, et al. Using Local Climate Zones in Sub-Saharan Africa to tackle urban health issues. Urban Climate. (2019); 27:227–42. Available from: https://doi.org/10.1016/j.uclim.2018.12.004

Chavez PS. An improved dark-object subtraction technique for atmospheric scattering correction of multispectral data. Remote Sensing of Environment (1988); 24:459–79.

Congedo L. Semi-Automatic Classification Plugin Documentation Release 4.8.0.1. Release. (2016); 4:29. Available from: https://media.readthedocs.org/pdf/semiautomaticclassificationmanual-v4/latest/semiautomaticclassificationmanual-v4.pdf

De Ridder K, Lauwaet D, Maiheu B. UrbClim - A fast urban boundary layer climate model. Urban Climate. (2015); 12:21–48. Available from: http://dx.doi.org/10.1016/j.uclim.2015.01.001

Demuzere M, Kittner J, Martilli A, Mills G, Moede C, Stewart ID, et al. A global map of local climate zones to support earth system modelling and urban-scale environmental science. Earth System Science Data. (2022); 14:3835–73.

Diallo-Dudek J, Lacaze B, Comby J. Land surface temperature in the urban area of Lyon metropolis: A comparative study of remote sensing data and MesoNH model simulation. 2015 Joint Urban Remote Sensing Event, JURSE. (2015); 2–5.

Emmanuel R, Krüger E. Urban heat island and its impact on climate change resilience in a shrinking city: The case of Glasgow, UK. Building and Environment. (2012); 53:137–49. Available from: http://dx.doi.org/10.1016/j.buildenv.2012.01.020

Equere V, Mirzaei PA, Riffat S. Definition of a new morphological parameter to improve prediction of urban heat island. Sustainable Cities and Society. (2020) ;56.

Founda D, Santamouris M. Synergies between Urban Heat Island and Heat Waves in Athens (Greece), during an extremely hot summer (2012). Scientific Reports. (2017); 7:1–11. Available from: http://dx.doi.org/10.1038/s41598-017-11407-6

Geletič J, Lehnert M, Savić S, Milošević D. Modelled spatiotemporal variability of outdoor thermal comfort in local climate zones of the city of Brno, Czech Republic. Science of the Total Environment. (2018); 624:385–95.

Guo A, Yang J, Xiao X, Xia (Cecilia) J, Jin C, Li X. Influences of urban spatial form on urban heat island effects at the community level in China. Sustainable Cities and Society. (2020); 53:101972. Available from: https://doi.org/10.1016/j.scs.2019.101972

Hass AL, Ellis KN, Mason LR, Hathaway JM, Howe DA. Heat and humidity in the city: Neighborhood heat index variability in a mid-sized city in the Southeastern United States. International Journal of Environmental Research and Public Health. (2016); 13.

Hidalgo García D, Arco Díaz J. Modeling of the Urban Heat Island on local climatic zones of a city using Sentinel 3 images: Urban determining factors. Urban Climate (2021); 37.

Hua L, Zhang X, Nie Q, Sun F, Tang L. The impacts of the expansion of urban impervious surfaces on urban heat islands in a coastal city in China. Sustainability. (2020); 12.

IPCC. The fifth report of the Intergovernmental Panel on Climate Change (IPCC). [Internet]. (2013). Available from: https://www.ipcc.ch/report/ar5/wg1/

Jacobs C, Singh T, Gorti G, Iftikhar U, Saeed S, Syed A, et al. Patterns of outdoor exposure to heat in three South Asian cities. Science of the Total Environment. (2019); 674:264–78. Available from: https://doi.org/10.1016/j.scitotenv.2019.04.087

Kafy A Al, Faisal A Al, Rahman MS, Islam M, Al Rakib A, Islam MA, et al. Prediction of seasonal urban thermal field variance index using machine learning algorithms in Cumilla, Bangladesh. Sustainable Cities and Society. (2021);64: 102542. Available from: https://doi.org/10.1016/j.scs.2020.102542

Karakuş CB. The Impact of Land Use/Land Cover (LULC) Changes on Land Surface Temperature in Sivas City Center and Its Surroundings and Assessment of Urban Heat Island. Asia-Pacific Journal of Atmospheric Sciences. (2019); 55:669–84.

Khamchiangta D, Dhakal S. Physical and non-physical factors

driving urban heat island: Case of Bangkok Metropolitan Administration, Thailand. Journal of Environmental Management. (2019); 248:109285. Available from: https://doi.org/10.1016/j.jenvman.2019.109285

Kotharkar R, Ghosh A, Kotharkar V. Estimating summertime heat stress in a tropical Indian city using Local Climate Zone (LCZ) framework. Urban Climate. (2021); 36.

Kovats RS, Campbell-Lendrum D, Matthies F. Climate change and human health: Estimating avoidable deaths and disease. Risk Analysis. (2005); 25:1409–18.

Kumar P, Rai A, Upadhyaya A, Chakraborty A. Analysis of heat stress and heat wave in the four metropolitan cities of India in recent period. Science of the Total Environment. (2022); 818.

Li B, Tao S, Dawson RW. Relations between AVHRR NDVI and ecoclimatic parameters in China. International Journal of Remote Sensing. (2002); 23: 989–99.

Li J, Song C, Cao L, Zhu F, Meng X, Wu J. Impacts of landscape structure on surface urban heat islands: A case study of Shanghai, China. Remote Sensing of Environment. (2011); 115:3249–63.

Martí Ezpeleta A, Royé D. Intensidad y duración del estrés térmico en verano en el área urbana de Madrid. Geographicalia. (2021); 95–113.

Mora C, Dousset B, Caldwell IR, Powell FE, Geronimo RC, Bielecki CR, et al. Global risk of deadly heat. Nature Climate Change. (2017); 7:501–6.

Nicholson SE, Farrar TJ. The influence of soil type on the relationships between NDVI, rainfall, and soil moisture in semiarid Botswana. I. NDVI response to rainfall. Remote Sensing of Environment. (1994); 50:107–20.

Rothfusz LP, Headquarters NSR. The heat index equation (or, more than you ever wanted to know about heat index). Fort Worth, Texas: National Oceanic and Atmospheric Administration, National Weather Service, Office of Meteorology. (1990); 23–90. Available from: papers://c6bd9143-3623-4d4f-963f-62942ed32f11/Paper/p395

Royé D, Sera F, Tobías A, Lowe R, Gasparrini A, Pascal M, et al. Effects of Hot Nights on Mortality in Southern Europe. Epidemiology. (2021); 487–98.

Rozenstein O, Qin Z, Derimian Y, Karnieli A. Derivation of land surface temperature for landsat-8 TIRS using a split window algorithm. Sensors (2014); 14:5768–80.

Santamouris M. Recent progress on urban overheating and heat island research. Integrated assessment of the energy, environmental, vulnerability and health impact. Synergies with the global climate change. Energy and Buildings. (2020); 207.

Schneider A, Friedl MA, Potere D. Mapping global urban areas using MODIS 500-m data: New methods and datasets based on "urban ecoregions." Remote Sensing of Environment. (2010); 114:1733–46.

Song J, Chen W, Zhang J, Huang K, Hou B, Prishchepov A V. Effects of building density on land surface temperature in China: Spatial patterns and determinants. Landscape and Urban Planning. (2020); 198:103794. Available from: https://doi.org/10.1016/j.landurbplan.2020.103794

Stewart ID, Oke TR. Local climate zones for urban temperature studies. Bulletin of the American Meteorological Society. (2012); 93:1879–900.

UNO. 68% of the world population projected to live in urban areas by 2050, says UN. (2018); Available from: https://www.un.org/development/desa/en/news/population/2018-revision-of-world-urbanization-prospects.html

Verdonck ML, Demuzere M, Hooyberghs H, Beck C, Cyrys J, Schneider A, et al. The potential of local climate zones maps as a heat stress assessment tool, supported by simulated air temperature data. Landscape and Urban Planning. (2018); 178:183–97. Available from: https://doi.org/10.1016/j.landurbplan.2018.06.004

Wang T, Shi J, Ma Y, Husi L, Comyn-Platt E, Ji D, et al. Recovering Land Surface Temperature Under Cloudy Skies Considering the Solar-Cloud-Satellite Geometry: Application to MODIS and Landsat-8 Data. Journal of Geophysical Research: Atmospheres. (2019); 124:3401–16.

Wang J, Ouyang W. Attenuating the surface Urban Heat Island within the Local Thermal Zones through land surface modification. Journal of Environmental Management. (2017); 187:239–52. Available from: http://dx.doi.org/10.1016/j.jenvman.2016.11.059

Yang C, Yan F, Zhang S. Comparison of land surface and air temperatures for quantifying summer and winter urban heat island in a snow climate city. Journal of Environmental Management. (2020); 265: 110563. Available from: https://doi.org/10.1016/j.jenvman.2020.110563

Zha Y, Gao J, Ni S. Use of normalized difference built-up index in automatically mapping urban areas from TM imagery. International Journal of Remote Sensing (2003); 24:583–94.

Zhang Y, Chen L, Wang Y, Chen L, Yao F, Wu P, et al. Research on the contribution of urban land surface moisture to the alleviation effect of urban land surface heat based on landsat 8 data. Remote Sensing. (2015); 7:10737–62.

Zhou D, Zhao S, Zhang L, Sun G, Liu Y. The footprint of urban heat island effect in China. Scientific Reports. (2015); 5:2–12.